

Neurology®

A new early and automated MRI-based predictor of motor improvement after stroke

Cristina Granziera, Alessandro Daducci, Djalel E. Meskaldji, et al.
Neurology 2012;79;39; Published online before print June 20, 2012;
DOI 10.1212/WNL.0b013e31825f25e7

This information is current as of July 3, 2013

The online version of this article, along with updated information and services, is located on the World Wide Web at:
<http://www.neurology.org/content/79/1/39.full.html>

Neurology ® is the official journal of the American Academy of Neurology. Published continuously since 1951, it is now a weekly with 48 issues per year. Copyright © 2012 American Academy of Neurology. All rights reserved. Print ISSN: 0028-3878. Online ISSN: 1526-632X.



A new early and automated MRI-based predictor of motor improvement after stroke

Cristina Granziera, MD,

PhD

Alessandro Daducci, PhD

Djalel E. Meskaldji

Alexis Roche, PhD

Philippe Maeder, MD

Patrik Michel, MD

Nouchine Hadjikhani,
MD, PhD

A. Gregory Sorensen, MD

Richard S. Frackowiak,
MD

Jean-Philippe Thiran, PhD

Reto Meuli, MD, PhD

Gunnar Krueger, PhD

Correspondence & reprint
requests to Dr. Granziera:
cristina.granziera@chuv.ch

ABSTRACT

Objectives: In this study, we investigated the structural plasticity of the contralesional motor network in ischemic stroke patients using diffusion magnetic resonance imaging (MRI) and explored a model that combines a MRI-based metric of contralesional network integrity and clinical data to predict functional outcome at 6 months after stroke.

Methods: MRI and clinical examinations were performed in 12 patients in the acute phase, at 1 and 6 months after stroke. Twelve age- and gender-matched controls underwent 2 MRIs 1 month apart. Structural remodeling after stroke was assessed using diffusion MRI with an automated measurement of generalized fractional anisotropy (GFA), which was calculated along connections between contralesional cortical motor areas. The predictive model of poststroke functional outcome was computed using a linear regression of acute GFA measures and the clinical assessment.

Results: GFA changes in the contralesional motor tracts were found in all patients and differed significantly from controls ($0.001 \leq p < 0.05$). GFA changes in intrahemispheric and interhemispheric motor tracts correlated with age ($p \leq 0.01$); those in intrahemispheric motor tracts correlated strongly with clinical scores and stroke sizes ($p \leq 0.001$). GFA measured in the acute phase together with a routine motor score and age were a strong predictor of motor outcome at 6 months ($r^2 = 0.96$, $p = 0.0002$).

Conclusion: These findings represent a proof of principle that contralesional diffusion MRI measures may provide reliable information for personalized rehabilitation planning after ischemic motor stroke. *Neurology*® 2012;79:39–46

GLOSSARY

Cd = Cook distance; **DSI** = diffusion spectrum imaging; **DTI** = diffusion tensor imaging; **FA** = fractional anisotropy; **FIM** = Functional Independence Measure; **FOV** = field of view; **GFA** = generalized fractional anisotropy; **GLM** = general linear model; **M1** = primary motor area; **MANOVA** = multivariate analysis of variance; **MPRAGE** = magnetization-prepared rapid gradient echo; **mRS** = modified Rankin Scale; **NIHSS** = NIH Stroke Scale; **PMd** = dorsal premotor area; **PMv** = ventral premotor area; **TE** = echo time; **tp** = time point; **TR** = repetition time.

Neuroimaging studies have provided an invaluable window into poststroke recovery human brain plasticity and shown that both contralateral cortical networks and contralesional descending pathways remodel after stroke.^{1–11}

In the 1990s, PET experiments in recovered hemiparetic patients evidenced motor activity-induced brain activations in a number of nonprimary motor regions both in lesioned and contralesional hemispheres.^{1–3} fMRI studies subsequently demonstrated that the amount of contralesional activation was highly dependent on the degree of patient impairment and brain damage.^{5,6,8} More recently, a study using EEG, PET, and transcranial magnetic stimulation showed enhanced recruit-

Supplemental data at
www.neurology.org



From the Departments of Clinical Neurosciences (C.G., P.M., R.S.F.) and Radiology (P.M., J.-P.T., R.M.), Centre Hospitalier Universitaire Vaudois and University of Lausanne, Lausanne; STI/IEL/LTS5 (A.D., D.E.M., J.-P.T.), EPFL, Lausanne; Advanced Clinical Imaging and Technology Group (A.R., C.G., G.K.), CIBM, EPFL, Lausanne; GRHAD (N.H.), BMI, SV, EPFL, Lausanne, Switzerland; Radiology (N.H., A.G.S.), Martinos Center for Biomedical Imaging, MGH, Boston, MA; Siemens Switzerland Healthcare IM S AW (G.K.), Renens, VD, Switzerland; and Siemens Healthcare North America (G.S.), Malvern, PA.

Study funding: Supported by Centre d'Imagerie BioMédicale of the University of Lausanne, the Swiss Federal Institute of Technology Lausanne, the University of Genève, the Centre Hospitalier Universitaire Vaudois, the Hôpitaux Universitaires de Genève, the Leenaards, the Jeantet and the Stoicescu Foundations, and the Swiss National Science Foundation Grant PZ00P3_131914/1. The funding source had no role in study design, in the collection, analysis, and interpretation of data, in the writing of the report, or in the decision to submit the article for publication.

Go to Neurology.org for full disclosures. Disclosures deemed relevant by the authors, if any, are provided at the end of this article.

ment of the contralateral sensorimotor cortex after subcortical stroke.⁹ In addition, diffusion tensor imaging (DTI) revealed that well-recovered chronic stroke patients relative to controls had elevated fractional anisotropy (FA) in both ipsilesional and contralateral corticospinal tracts¹⁰ and an increase or decrease of specific fiber trajectories connecting cortical regions in both hemispheres.¹¹

However, no study has specifically focused on structural motor network remodeling in stroke patients with motor deficits, although motor deficits are a major cause of disability.¹²

To determine the importance of such contralateral structural changes in recovering stroke patients, we imaged longitudinally a patient cohort with motor deficits using diffusion spectrum imaging (DSI) MRI.

We aimed to explore whether 1) contralateral structural changes after stroke can be detected with DSI-based metrics; 2) repeated DSI measurements correlate with clinical scores, stroke size, age, or gender; and 3) DSI-based metrics and clinical status can predict motor outcome.

METHODS We enrolled 12 patients (7 male and 5 female) with ischemic infarction affecting the motor cortex or subcortical structures involved in motor control. Patients with brainstem and cerebellar infarcts were excluded from the study as well as patients with massive edema provoking midline shift. The mean age and SD was 58.4 ± 17.0 years.

All patients underwent 3 DSI scans 1) within 1 week (time point [tp] 1), 2) at 1 month (± 1 week, tp2), and 3) at 6 months (± 15 days, tp3) after stroke, the period when most functional improvement occurs.¹³ Twelve age- and gender-matched healthy con-

trols (57.2 ± 14.5 years, mean \pm SD) were also included in the study and underwent 2 DSI scans 1 month apart (tp1c and tp2c). DSI resolves complex crossing and kissing of axonal bundles as well as the intersections of white matter fibers in cortical and deep gray matter structures¹⁴ and is therefore appropriate for mapping networks in the context of functional improvement.

Patients had no history of previous stroke or other neurologic, psychiatric, or major systemic illnesses. They all received antiplatelet treatment and underwent standard rehabilitation programs, as performed in the University Hospital of Lausanne. None used antidepressant or CNS stimulator drugs during rehabilitation.

Standard protocol approvals, registrations, and patient consents. All subjects provided written informed consent prior to imaging and the Lausanne University Hospital review board approved the study protocol.

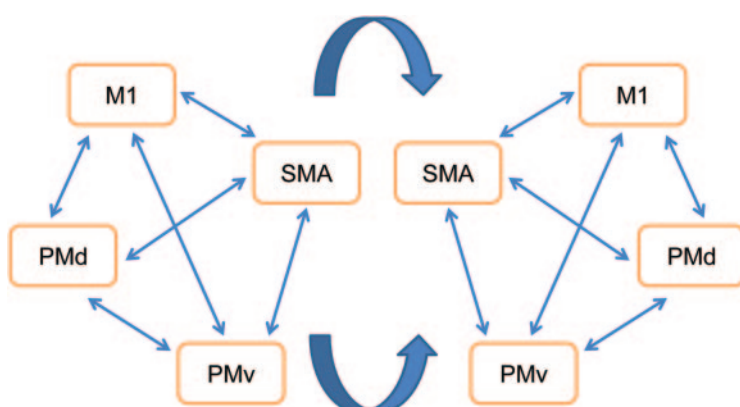
Clinical assessment. Patients underwent clinical assessments (NIH Stroke Scale [NIHSS], Functional Independence Measure [FIM], and modified Rankin Scale [mRS] scores) at each time point. The motor part of the NIHSS score (NIHSS motor¹⁵) was derived from items 2 to 7 and 10 (<http://www.nihstroke.org/>). Items 2 (gaze), 4 (facial palsy), 7 (ataxia), and 10 (dysarthria) were included as they were considered to be a consequence of hemispheric lesions given that patients with brainstem or cerebellar lesions were excluded. Patient demographics and presumed etiologic stroke mechanisms¹⁶ were obtained from medical records and standardized workup in the stroke unit.

Image acquisition and analysis. All DSI measurements (repetition time [TR]/echo time [TE] = 6,600/138 msec, field of view [FOV] = 212×212 mm, 34 slices, $2.2 \times 2.2 \times 3$ mm resolution, 258 diffusion directions, $b = 8,000$ s/mm²) were performed at 3T (Magnetom Trio a Tim System, Siemens, Erlangen, Germany) using a 32-channel head matrix coil (for a detailed explanation of the method, see reference 17). Orientation distribution functions were reconstructed using the Diffusion Toolkit (www.trackvis.org/dtk). Fiber-tracking was performed via a streamline algorithm (www.cmtk.org). High-resolution magnetization-prepared rapid gradient echo (MPRAGE) images (TR/TE = 2,400/3 msec, voxel = $1 \times 1 \times 1.2$ mm, FOV = 256×240 mm, generalized autocalibrating partially parallel acquisition [GRAPPA] = 2)¹⁷ were acquired for anatomic reference and linearly registered to T2 images (TR/TE = 3,000/84 msec, voxel = $0.5 \times 0.5 \times 3$ mm).

To account for spatial distortions in the EPI readout, a non-linear registration was used to register the T2 to the diffusion-weighted image volumes ($b = 0$ s/mm²). All registrations were performed using FSL (www.fmrib.ox.ac.uk/fsl). Motor cortical regions in the contralateral hemisphere were mapped from MPRAGE images using Freesurfer (www.surfer.nmr.mgh.harvard.edu); intrahemispheric and interhemispheric connections (figure 1) were identified to allow clustering of all fiber trajectories between 1) pairs of motor areas in the contralateral hemisphere and 2) each contralateral motor area and the corpus callosum. The connectivity between 2 motor areas was indexed by mean tract GFA, which was obtained by averaging the GFA calculated in every single point constituting each fiber trajectory. The same analysis was performed in healthy subjects in both hemispheres and averages were performed between left and right GFA values for each tract at each time point.

In addition, intrahemispheric and interhemispheric connectivity among visual areas (V1–V2–V3) was calculated in the

Figure 1 Schematic representation of the motor network and motor-associated connections (white matter tracts)



The thin arrows indicate intrahemispheric connections and the thick arrows indicate interhemispheric connections. M1 = primary motor area; PMd = premotor dorsal area; PMv = premotor ventral area; SMA = supplementary motor area.

Downloaded from www.neurology.org at Harvard University on July 3, 2013

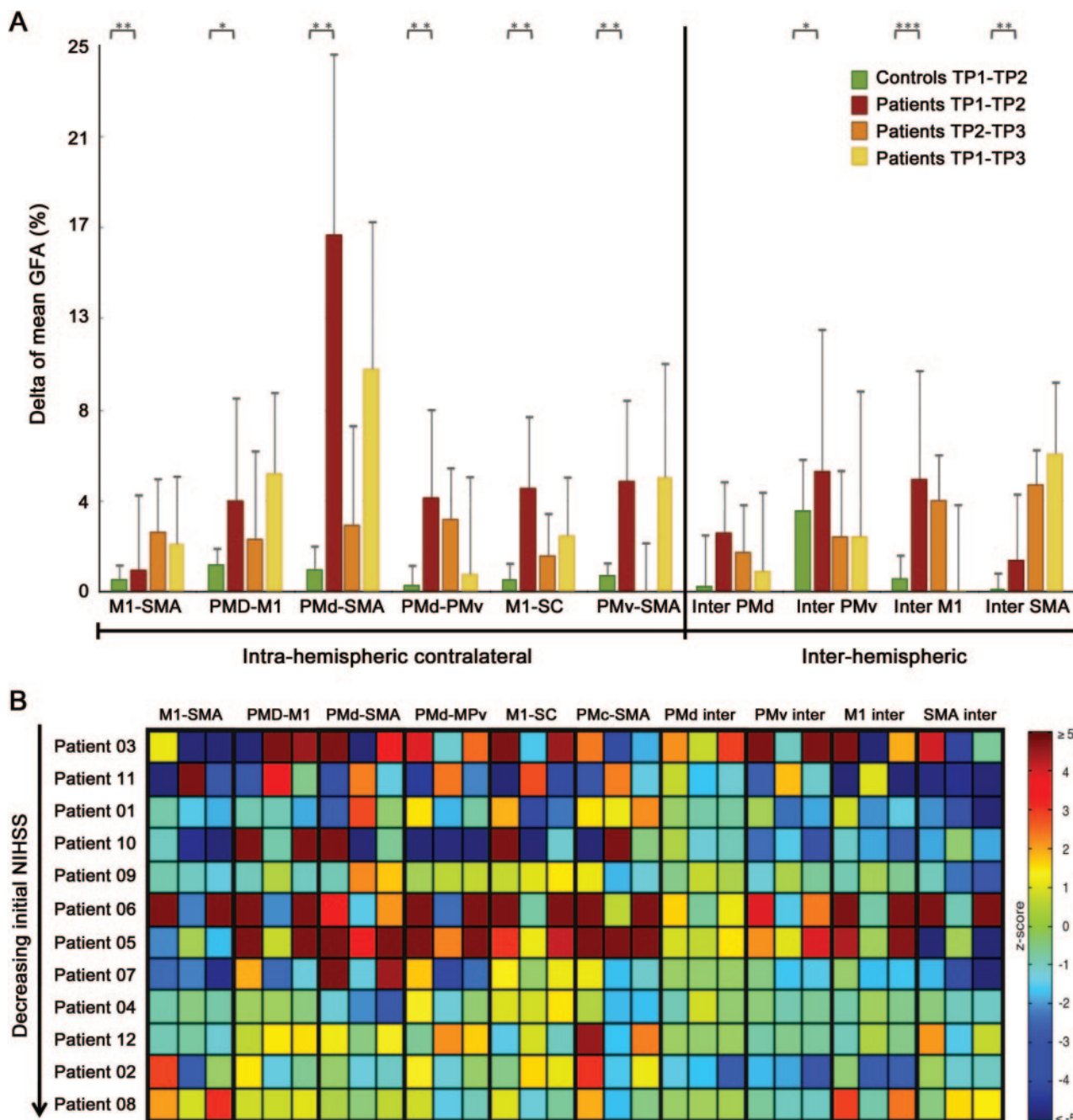
same way for comparison, assuming that the strokes had not affected the visual pathways. The entire tractographic analysis was performed in a fully automated manner (www.cmtk.org). Stroke lesion volumes were evaluated on MPRAGE images using in-house software.

Metrics and statistical analysis. GFA is a measure of anisotropy of the local diffusion profile (orientation density function) obtained in high angular resolution diffusion MRI experi-

ments.¹⁸ It is described as the SD along the different diffusion directions, each of them representing fiber trajectory in tractography reconstructions.¹⁹

Statistical analysis was performed using multivariate analysis of variance (MANOVA) to compare 1) intrahemispheric and interhemispheric motor and visual tract GFA in patients and controls at tp1 and 2) absolute GFA changes between serial scans in patients. In this context, we use the word “absolute” to indi-

Figure 2 Generalized fractional anisotropy (GFA) changes in patients and controls



(A) Delta of the mean absolute GFA changes between serial scans (time point [tp] 1 vs tp2, tp2 vs tp3, and tp1 vs tp3) calculated along the connections between motor areas in patients and controls. Significance value * $p < 0.05$; ** $p < 0.01$; *** $p < 0.001$. (B) Individual profiles of GFA changes between tp1 and tp2 (first column), tp2 and tp3 (second column), and tp1 and tp3 (third column) for each motor connection studied (primary motor area [M1]-supplementary motor area [SMA], dorsal premotor area [PMD]-M1, PMd-SMA, PMd-[PMv], M1-SC, PMv-SMA, PMd inter, PMv inter, M1 inter, SMA inter). GFA changes in each single patient were compared to the mean GFA changes in controls using z scores ($-5 \leq z \text{ score} \leq +5$). Patients are ordered according to the initial NIH Stroke Scale (NIHSS) (from severe deficits to mild on the y-axis).

Downloaded from www.neurology.org at Harvard University on July 3, 2013

cate real numbers without regard to its sign. The MANOVA used the GFA as the dependent variable, and age, NIHSS, mRS, and FIM as independent variables with 2 levels of factor: “patients” and “controls.”

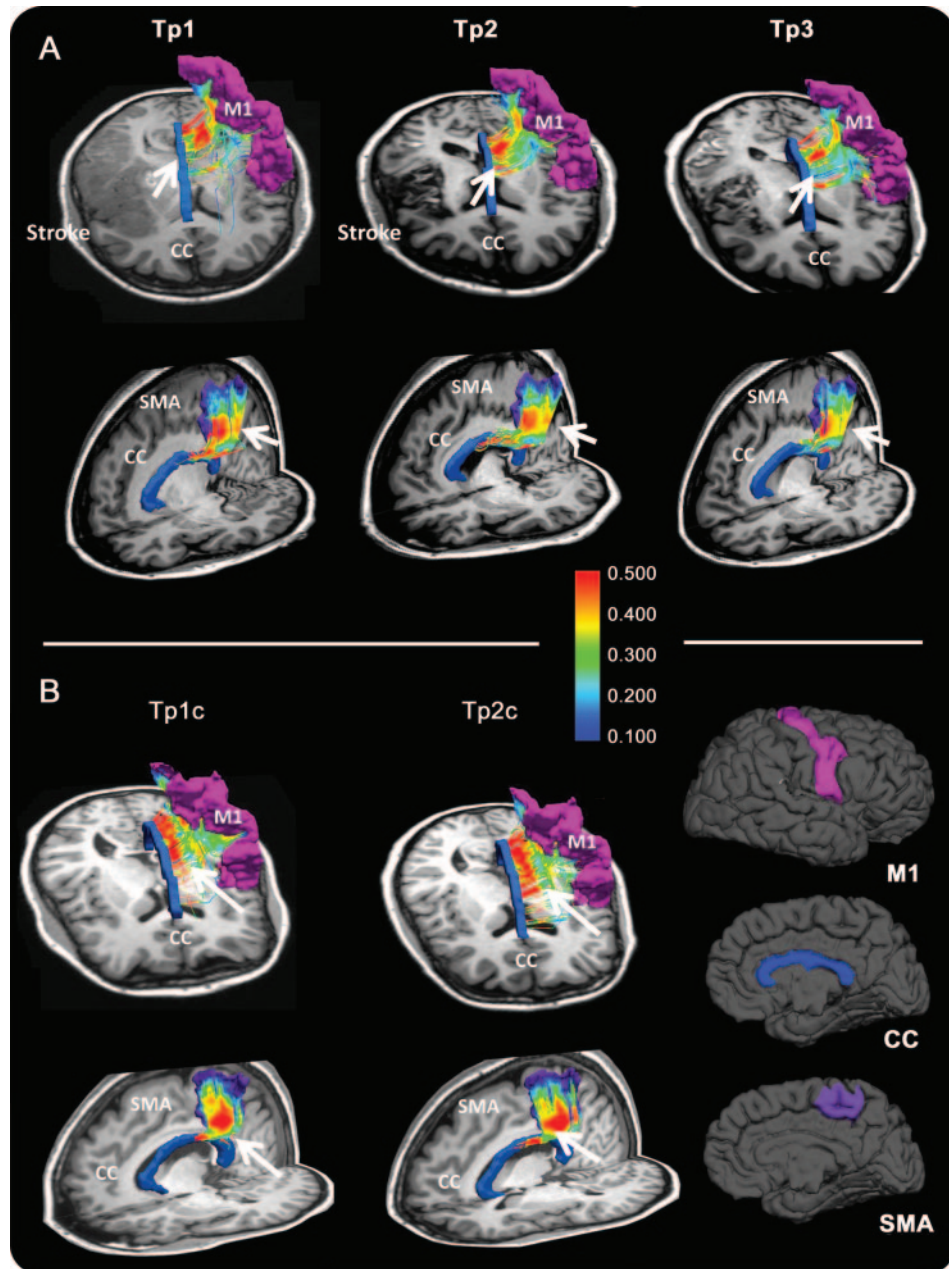
A general linear model (GLM) was applied to GFA changes between time points (tp1, tp2, and tp3), clinical scores, lesion volumes, and demographic information (age and gender).

In order to show the profile of GFA changes in each patient compared to healthy controls, *t* tests were performed comparing GFA changes measured in patients (tp2–tp1, tp3–

tp2, and tp3–tp1) and GFA variability computed in healthy controls (tp2c–tp1c).

The predictive value of the imaging indices was assessed by linear regression with clinical scores in the acute phase and at 6-month follow-up using demographic information (age), stroke size, GFA values, and NIHSS motor scores obtained at tp1 and tp2. A backward selection process was used to select the best prediction model with $p = 0.05$ as a threshold of significance. In order to estimate the influence of a data point in the model, we computed Cook distances (Cd); Cd < 4/n, where n is the num-

Figure 3 Diffusion spectrum imaging (DSI) tractography view of the interhemispheric connections between the primary motor area (M1) and the corpus callosum (CC) as well as between the supplementary motor area (SMA) and the corpus callosum (CC) in one hemisphere of control subject 6 (A) and in the contralateral healthy hemisphere of patient 6 (B)



Fiber trajectories are color coded using a scalar scale based on GFA (max value 0.5 and min value 0.1). Arrows indicate the absence of substantial differences between the time point (tp) 1c and tp2c (A); on the contrary, it is possible to observe a decrease in GFA in both M1-CC and SMA-CC connections between tp1 and tp2 and between tp2 and tp3.

Downloaded from www.neurology.org at Harvard University on July 3, 2013

ber of observations, indicate that a subject does not have an inordinately high influence on the model. In addition, a “leave-one-out test” was performed. This test is a cross-validation procedure that uses as a training dataset all the subjects excluding one at a time, who is considered the “test” set. The procedure is repeated a number of times so that each observation in the sample is used once as the test data. This technique is usually applied in order to assess how the results of a statistical analysis generalize to an independent dataset and to prevent against overfitting. Moreover, it gives statistically powerful information about the robustness of the significance of the obtained results.²⁰

All statistical analyses were performed using *R* software (www.r-project.org).

RESULTS Patient demographics, clinical characteristics, and functional scores are summarized in tables e-1 and e-2 on the *Neurology*[®] Web site at www.neurology.org. The average stroke size was $64.3 \pm 68.9 \text{ cm}^3$ (mean \pm SD).

Reproducibility of GFA measures in control subjects. In control subjects, the mean absolute GFA change obtained for intrahemispheric and interhemispheric motor connections between tp1c and tp2c was 0.0035 ± 0.0042 (mean \pm SEM). The greatest variability was seen in connections between the 2 PMv regions (figure 2A). Connections between the ventral premotor (PMv) and the primary motor (M1) areas were not analyzed due to poor visualization with DSI tractography.

Comparison of absolute GFA changes in patients and controls. In patients, absolute GFA changes in contralateral motor connections between tp1 and tp2 were significantly different from absolute GFA changes between the same regions in controls between tp1c and tp2c (figure 2A, $0.001 \leq p < 0.05$). Only connections between the 2 dorsal premotor areas (PMd) failed to show a significant GFA difference.

Longitudinal GFA changes in patients. Individual patients showed increased or decreased GFA in each investigated motor connection, with a pattern that appeared to be patient-specific (figures 2B and 3, A

and B). Compared to controls, however, GFA changes were greatest in patients with the more severe motor deficits (figure 2B).

Longitudinal evaluation of GFA changes in patients. No significant differences were observed when absolute GFA values were compared among time points in patients.

Correlation of absolute GFA changes with clinical scores in patients. MANOVA showed a strong correlation between patient absolute GFA changes for intrahemispheric motor connections in the contralateral hemisphere and 1) age ($p < 0.01$, $F_{4,6}$, residuals 28, df_4), 2) NIHSS motor ($p \leq 0.001$, $F_{6,1}$, residuals 28, df_4), and 3) stroke size ($p \leq 0.001$, $F_{6,2}$, residuals 28, df_4). Similarly, patient absolute GFA changes in interhemispheric connections were highly correlated with age ($p \leq 0.0001$, $F_{15,7}$, residuals 28, df_4).

A GLM analysis further clarified that only 13 out of the 30 (10×3) measurements of GFA evolution in the investigated motor tracts (tp1–tp2, tp2–tp3, tp1–tp3) were significantly correlated with clinical scores (NIHSS, NIHSS motor, mRS, FIM), stroke sizes, or patient ages ($0.0005 < p < 0.05$; for details, see supplementary data).

Individual patterns of GFA changes and GFA values at each time point did not exhibit any significant correlation with motor scores.

Prediction of clinical outcome in patients using GFA. In the patient cohort, a linear regression using a backward selection model including GFA data from the first time point (tp1) as well as age and NIHSS motor (tp1) was shown to predict the NIHSS motor at tp3 (6-month follow-up) with high significance (multiple $R^2 = 0.98$, adjusted $R^2 = 0.96$, $p = 0.0007$, table 1 and figure 4). The relative importance of NIHSS tp1, age, and GFA tp1 was evaluated with Fisher test and is shown in table 1. Inclusion of stroke size did not lead to any significant predictive power ($p = 0.1$). The Cook distances in all subjects were below 0.33, indicating the absence of outliers.

Table 1 Prediction of the NIHSS tp3 using a model based on the NIHSS scores at tp1, motor tract GFA values at tp1, and patient ages^a

Coefficients	Estimate	Standard error	t Value	p Value	Confidence interval
NIHSS (tp1)	0.31	0.06	4.79	0.002	0.12, 0.39
Age	0.05	0.02	3.19	0.015	0.004, 0.11
GFA M1-SMA (tp1)	58.61	12.54	4.67	0.002	43.32, 117.84
PMd-PMv (tp1)	-43.67	8.97	-4.87	0.002	-84.26, -89.72
SMA-SMA (tp1)	-30.57	8.12	-3.77	0.007	-64.45, -16.61

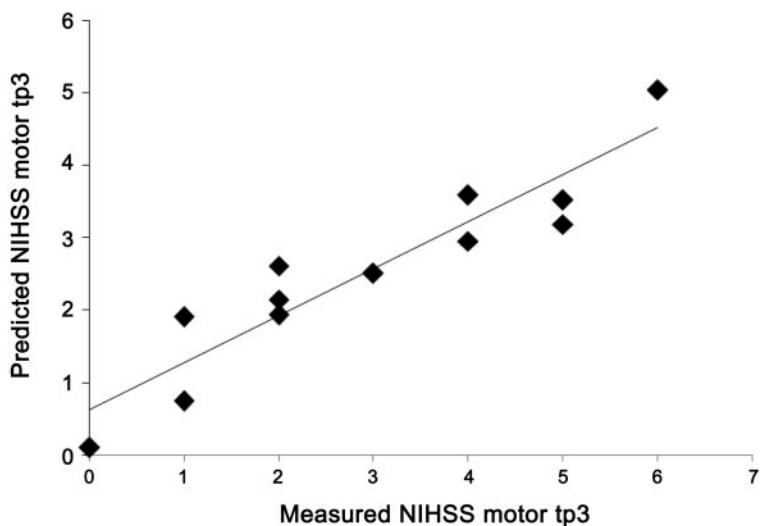
Abbreviations: GFA = generalized fractional anisotropy; NIHSS = NIH Stroke Scale; PMd = premotor dorsal area; PMv = premotor ventral area; SMA = supplementary motor area; tp = timepoint.

^a Residual standard error: 0.6727 on 6 df. Multiple R^2 : 0.9807, adjusted R^2 : 0.9615, F statistic: 50.93 on 6 and 6 df, $p = 0.0007$.

Downloaded from www.neurology.org at Harvard University on July 3, 2013

Figure 4

Graphical representation of the real and predicted NIH Stroke Scale (NIHSS) at time point 3 using the model reported in table 1



Likewise, a leave-one-out test including all subjects confirmed the robustness of the correlation between predicted and recorded NIHSS values at tp3 ($R^2 = 0.87$).

A model including only age and NIHSS motor at tp1 gave a lower correlation (multiple $R^2 = 0.83$, adjusted $R^2 = 0.81$) as did a model including only NIHSS tp1 (multiple $R^2 = 0.83$, adjusted $R^2 = 0.82$). A model including the GFA values at tp1 with age and another including GFA values only gave equal correlation values (multiple $R^2 = 0.88$, adjusted $R^2 = 0.84$). A model including the NIHSS motor score and GFA values showed a higher correlation but not as high as the model that also included patient ages (multiple $R^2 = 0.93$, adjusted $R^2 = 0.90$).

Specificity of the observed GFA changes in the motor network. The MANOVA analysis performed with visual areas failed to show any significant changes between tp1 and tp2 in patients and tp1c and tp2c.

DISCUSSION This longitudinal MRI study of motor stroke patients shows that contralesional structural changes in the motor network can be measured using DSI and that changes correlate with functional motor improvement. In addition, our findings strongly suggest that GFA at tp1, combined with patient age and the acute clinical NIHSS score, is an important predictor of motor improvement 6 months after stroke ($R^2 = 0.96$, $p = 0.0007$).

Our data confirm and extend the findings of recent studies providing arguments for a major role of contralesional white matter remodeling in poststroke functional improvement.^{5,9,10,21}

Thus far, most studies on contralesional plasticity have been performed in cohorts of patients with sub-

cortical or small strokes.^{5,9,10,21} In our work, we considered a population of patients with heterogeneous lesion size (table e-1) and we found that, independently of cortical or subcortical lesion location, patients show a significant degree of contralesional motor connection remodeling. This is consistent with previous studies showing a motor system-wide compensation that is independent of the site and size of stroke lesions.^{1,3,6,8}

Almost all studies examining the role of the contralesional hemisphere in poststroke functional improvement report functional data.^{1,3,5,6,8,9,21} Only recently a DTI-based network analysis at a single time point showed increases or decreases in the number of fiber trajectories between various contralateral regions compared to homologous regions in control subjects.¹¹ In our study, we investigated contralesional motor-associated structural plasticity at multiple time points over 6 months after stroke, because most functional improvement is found within this period.¹³ In addition, we correlated the observed changes with functional outcome and propose a predictive model of motor improvement after the acute event.

We obtained good reproducibility of our GFA measure along tracts associated with the motor network in controls (figure 2A). Despite the fact that the DSI technique is sensitive to complex fiber structures (fiber crossing, kissing) and remodeling mechanisms (axonal sprouting), it also appears sensitive to imperfections in acquisition (e.g., patient motion) and data postprocessing. Our results, however, indicate that clinically relevant information can be successfully extracted in an automatic fashion from high-quality data. The least reproducible results were found in tracts between the contralesional PMv and corpus callosum, presumably due to technical limitations of DSI with respect to the small size of PMv and the relatively long path that these connections follow to reach the corpus callosum.

One of our major findings is that changes in contralesional GFA of the motor network between time points 1 and 2 differed substantially between patients and healthy subjects (figure 2A) even though there was heterogeneity of individual patterns of GFA changes (figure 3, A and B, and 4). No significant changes were found in the contralateral visual network when patients were compared to controls, confirming that the observed GFA changes are specific for the motor network. Increases in GFA indicate higher diffusivity along a certain direction in a brain tissue volume (anisotropy) and may be due to axonal sprouting or new connections between motor areas.²²

Decreases in GFA point to lower diffusivity along a specific direction in the brain tissue and may be

caused by axonal degeneration.²³ Crofts et al.¹¹ reported a decrease in the integrity of connections between areas in the contralateral hemisphere in stroke patients that they hypothesized were due to degeneration of fiber tracts connected with the infarcted areas of brain.¹¹ In line with Crofts et al.,¹¹ we interpret our results by relating differential individual connectivity patterns associated with variability in stroke size and location to various sites and inferred degrees of secondary degenerative and regenerative phenomena.

Another major finding of our study is that GFA-based structural changes in the contralateral motor network, rather than in the studied individual motor tracts, are highly correlated with changes in clinical scores and depend on age and stroke size. The results are in line with recent functional studies suggesting that cortico-cortical connections, in addition to motor descending pathways like the cortico-spinal tract, play a pivotal role in motor improvement after stroke.^{5,6,9,24}

Most importantly, we present a predictor of post-stroke functional improvement that is early and independent of stroke size and location. A very recent study by Lindenberg et al.²⁵ attempted to predict the effect of 5 days of transcranial magnetic stimulation and intensive rehabilitation therapy in a group of stroke patients with chronic stroke (>5 months after the acute event) by using DTI-based metrics of ipsilesional corticospinal tracts and transcallosal fibers (adjusted R 0.77–0.87). Likewise, a fMRI study by Zarahn et al.²⁴ showed that combined measures of fMRI activation and an acute motor score (Fugl-Meyer score) better predicted motor improvement in patients with severe initial deficits compared to the clinical score alone. Our results show that DSI-derived metrics in the motor connections of the contralateral hemisphere permit improved prediction in the acute phase in patients with heterogeneous deficits, even in the context of standard rehabilitation therapy.

The presented prediction model represents a proof of principle that automatically computed measures (GFA), together with a simple clinical assessment (NIHSS motor) and demographics (patient age), may provide a powerful, easily applicable tool for the routine care of acute stroke patients. We acknowledge, however, that our model was tested in a carefully selected cohort of relatively young patients (58.4 ± 17.0 years) and excluded subjects with previous strokes, posterior circulation infarcts, and large strokes with major edema. Future studies should broaden the inclusion criteria and include a higher number of patients over 65 since stroke prevalence increases markedly with age.²⁶ To test

whether these promising findings can be extended to wider clinical use.

Diffusion MRI is very helpful in the early diagnosis of stroke²⁷ and advanced diffusion techniques like DSI may aid in the future to establish personalized rehabilitation therapies like noninvasive brain stimulation²⁸ and robotics-based rehabilitation.²⁹ If reproduced in larger prospective studies, this advance may help to improve treatment and rehabilitation plans for stroke patients.

AUTHOR CONTRIBUTIONS

Study design (C.G., G.K., R.M., G.S.); collection, analysis, and interpretation of data (A.D., D.M., A.R., M.P., P.M., R.F., J.-P.T.); writing of the report and decision to submit the paper for publication (C.G., G.K., R.M., G.S., R.F., N.H., A.D., D.M., A.R., M.P., P.M., J.-P.T.).

ACKNOWLEDGMENT

The authors thank Dr. Xavier Gigandet and Dr. Leila Cammoun for suggestions in data processing, Dr. Bogdan Draganski for stroke lesions segmentation, and Nicolas Chevrey for help with data acquisition.

DISCLOSURE

C. Granziera, A. Daducci, D. Meskaldij, A. Roche, P. Maeder, P. Michel, and N. Hadjikhani report no disclosures. A.G. Sorensen is an employee of Siemens AG. R. Frackowiak, J.-P. Thiran, and R. Meuli report no disclosures. G. Krueger is an employee of Siemens AG. [Go to Neurology.org for full disclosures.](#)

Received December 13, 2011. Accepted in final form February 17, 2012.

REFERENCES

1. Weiller C, Chollet F, Friston KJ, Wise RJ, Frackowiak RS. Functional reorganization of the brain in recovery from striatocapsular infarction in man. Ann Neurol 1992;31:463–472.
2. Weiller C, Ramsay SC, Wise RJ, Friston KJ, Frackowiak RS. Individual patterns of functional reorganization in the human cerebral cortex after capsular infarction. Ann Neurol 1993;33:181–189.
3. Chollet F, DiPiero V, Wise RJ, Brooks DJ, Dolan RJ, Frackowiak RS. The functional anatomy of motor recovery after stroke in humans: a study with positron emission tomography. Ann Neurol 1991;29:63–71.
4. Rehme AK, Fink GR, von Cramon DY, Grefkes C. The role of the contralateral motor cortex for motor recovery in the early days after stroke assessed with longitudinal fMRI. Cereb Cortex Epub 2010.
5. Riecker A, Groschel K, Ackermann H, Schnaudigel S, Kasubek J, Kastrup A. The role of the unaffected hemisphere in motor recovery after stroke. Hum Brain Mapp 2010;31:1017–1029.
6. Ward NS, Brown MM, Thompson AJ, Frackowiak RS. Neural correlates of motor recovery after stroke: a longitudinal fMRI study. Brain 2003;126:2476–2496.
7. Ward NS, Brown MM, Thompson AJ, Frackowiak RS. Longitudinal changes in cerebral response to proprioceptive input in individual patients after stroke: an fMRI study. Neurorehabil Neural Repair 2006;20:398–405.
8. Ward NS, Newton JM, Swayne OB, et al. Motor system activation after subcortical stroke depends on corticospinal system integrity. Brain 2006;129:809–819.

9. Gerloff C, Bushara K, Sailer A, et al. Multimodal imaging of brain reorganization in motor areas of the contralateral hemisphere of well recovered patients after capsular stroke. *Brain* 2006;129:791–808.
10. Schaechter JD, Fricker ZP, Perdue KL, et al. Microstructural status of ipsilesional and contralateral corticospinal tract correlates with motor skill in chronic stroke patients. *Hum Brain Mapp* 2009;30:3461–3474.
11. Crofts JJ, Higham DJ, Bosnell R, et al. Network analysis detects changes in the contralateral hemisphere following stroke. *Neuroimage* 2011;54:161–169.
12. Cramer SC. Changes in motor system function and recovery after stroke. *Restor Neurol Neurosci* 2004;22:231–238.
13. Langhorne P, Coupar F, Pollock A. Motor recovery after stroke: a systematic review. *Lancet Neurol* 2009;8:741–754.
14. Wedeen VJ, Hagmann P, Tseng WY, Reese TG, Weisskoff RM. Mapping complex tissue architecture with diffusion spectrum magnetic resonance imaging. *Magn Reson Med* 2005;54:1377–1386.
15. Chollet F, Tardy J, Albucher JF, et al. Fluoxetine for motor recovery after acute ischaemic stroke (FLAME): a randomised placebo-controlled trial. *Lancet Neurol* 2011;10:123–130.
16. Ay H, Benner T, Arsava EM, et al. A computerized algorithm for etiologic classification of ischemic stroke: the Causative Classification of Stroke System. *Stroke* 2007;38:2979–2984.
17. Granziera C, Schmahmann JD, Hadjikhani N, et al. Diffusion spectrum imaging shows the structural basis of functional cerebellar circuits in the human cerebellum in vivo. *PLoS One* 2009;4:e5101.
18. Tuch DS. Q-ball imaging. *Magn Reson Med* 2004;52:1358–1372.
19. Johansen-Berg H, Behrens TEJ, eds. *Diffusion MRI: From Quantitative Measurements to In-vivo Neuroanatomy*. Academic Press; 2009.
20. Geisser S, ed. *Predictive Inference*. New York: Chapman and Hall; 1993.
21. Lotze M, Markert J, Sauseng P, Hoppe J, Plewnia C, Gerloff C. The role of multiple contralateral motor areas for complex hand movements after internal capsule lesion. *J Neurosci* 2006;26:6096–6102.
22. Granziera C, D'Arceuil H, Zai L, Magistretti PJ, Sorensen AG, de Crespigny AJ. Long-term monitoring of post-stroke plasticity after transient cerebral ischemia in mice using *in vivo* and *ex vivo* diffusion tensor MRI. *Open Neuroimag J* 2007;1:10–17.
23. Pierpaoli C, Barnett A, Pajevic S, et al. Water diffusion changes in Wallerian degeneration and their dependence on white matter architecture. *Neuroimage* 2001;13:1174–1185.
24. Zarahn E, Alon L, Ryan SL, et al. Prediction of Motor Recovery Using Initial Impairment and fMRI 48 h Post-stroke. *Cereb Cortex* Epub 2011.
25. Lindenberg R, Zhu LL, Ruber T, Schlaug G. Predicting functional motor potential in chronic stroke patients using diffusion tensor imaging. *Hum Brain Mapp* 2011.
26. Rosamond W, Flegal K, Furie K, et al. Heart disease and stroke statistics: 2008 update: a report from the American Heart Association Statistics Committee and Stroke Statistics Subcommittee. *Circulation* 2008;117:e25–e146.
27. Albers GW, Thijs VN, Wechsler L, et al. Magnetic resonance imaging profiles predict clinical response to early reperfusion: the diffusion and perfusion imaging evaluation for understanding stroke evolution (DEFUSE) study. *Ann Neurol* 2006;60:508–517.
28. Williams JA, Imamura M, Fregnani F. Updates on the use of non-invasive brain stimulation in physical and rehabilitation medicine. *J Rehabil Med* 2009;41:305–311.
29. Huang VS, Krakauer JW. Robotic neurorehabilitation: a computational motor learning perspective. *J Neuroeng Rehabil* 2009;6:5.

Visit the *Neurology®* Resident & Fellow Web Site

Click on Residents & Fellows tab at www.neurology.org.

Now offering:

- *Neurology®* Resident & Fellow Editorial team information
- “Search by subcategory” option
- E-pearl of the Week
- RSS Feeds
- Direct links to *Continuum®*, Career Planning, and AAN Resident & Fellow pages
- Recently published Resident & Fellow articles
- Podcast descriptions



[Find *Neurology®* on Facebook: http://tinyurl.com/neurologyfan](http://tinyurl.com/neurologyfan)



[Follow *Neurology®* on Twitter: http://twitter.com/GreenJournal](http://twitter.com/GreenJournal)

A new early and automated MRI-based predictor of motor improvement after stroke

Cristina Granziera, Alessandro Daducci, Djalel E. Meskaldji, et al.

Neurology 2012;79:39; Published online before print June 20, 2012;

DOI 10.1212/WNL.0b013e31825f25e7

This information is current as of July 3, 2013

Updated Information & Services	including high resolution figures, can be found at: http://www.neurology.org/content/79/1/39.full.html
Supplementary Material	Supplementary material can be found at: http://www.neurology.org/content/suppl/2012/06/21/WNL.0b013e31825f25e7.DC1.html
References	This article cites 24 articles, 7 of which can be accessed free at: http://www.neurology.org/content/79/1/39.full.html#ref-list-1
Subspecialty Collections	This article, along with others on similar topics, appears in the following collection(s): All Cerebrovascular disease/Stroke http://www.neurology.org/cgi/collection/all_cerebrovascular_disease_stroke DWI http://www.neurology.org/cgi/collection/dwi MRI http://www.neurology.org/cgi/collection/mri
Permissions & Licensing	Information about reproducing this article in parts (figures, tables) or in its entirety can be found online at: http://www.neurology.org/misc/about.xhtml#permissions
Reprints	Information about ordering reprints can be found online: http://www.neurology.org/misc/addir.xhtml#reprintus

